

NATURAL CONVECTION FROM SINGLE FINNED TUBE IMMERSSED IN A TILTED ENCLOSURE

Ass.Prof.Dr.Ikhlas M. Fayed, Hadi R. Roomi
University of Technology / Mech. Eng. Dept.

ABSTRACT

Heat transfer rates of a single horizontal finned tube immersed in water –filled enclosure tilted at 30 degrees are measured .The results serve as a baseline case for a solar water heating system with a heat exchanger immersed in integral collector storage. Tests were made with both adiabatic and uniform heat flux boundary conditions. Natural convection flow in enclosure is interpreted from measured water temperature distributions. Formation of an appropriate temperature difference that drives natural convection is determined .Correlations for the overall heat transfer coefficient in terms of the Nusselt and Rayleigh numbers are reduced to the form $Nu = 0.716Ra^{0.247}$

For $2 \times 10^5 \leq Ra \leq 2 \times 10^7$ Based on the diameter of the immersed tube .Comparison the present work results with others gave a good agreement.

KEY WORDS: Solar energy, Natural convection, Heat exchanger

الخلاصة:

قيس معدل انتقال الحرارة من أنبوب منفرد مغمور في ماء داخل مغلف . المغلف مائل عن الأفق بزاوية 30° . ممكن تمثيل النتائج لمنظومة تسخين بالطاقة الشمسية لمبادل حراري مغمور في مجمع الطاقة الشمسية أجريت الاختبارات لحالة العزل الحراري من جميع الجهات بوجود شروط حدية بثبوت درجة حرارة المائع مرة والحالة الثانية العزل الحراري من جميع الجهات ما عدا السطح العلوي إذ يتعرض لثبوت الفيض الحراري ممكن تمثيل جريان انتقال الحرارة بالحمل الحر داخل المغلف من خلال قياس درجات الحرارة داخله . العلاقة التجريبية لانتقال الحرارة بالحمل الحر ممكن تمثيلها بدلالة عدد نسلت ورقم رايلي من خلال العلاقة التجريبية التالية:

$$Nu=0.716Ra^{0.247} \quad \text{for } 2 \times 10^5 \leq Ra \leq 2 \times 10^7$$

قيست العلاقة على أساس قطر الأنبوب المغمور. قورنت نتائج البحث الحالي مع بحوث سابقة وحصل على توافق جيد.

INTRODUCTION

One obstacle to the wide spread use of solar water heating systems is either high initial cost .A potential method of reducing cost is to use components made of plastic rather than metal .One system concept **Fig.1** embodies an expensive bag for collection and storage .An immersed heat exchanger made of many tubes transfers the stored energy to the potable water circulated through the tubes. The heat transfer process in the collector and immersed heat exchanger **Fig.2** involves the interaction of negatively buoyant plumes within the tube bundle and a large –scale buoyant flow within the collector. Natural convection heat transfer characteristics from horizontal tube in an unbounded fluid have been studied extensively .(Morgan 1975) assembled the widely disparate data and proposed Nusselt versus Ralyeigh number correlations .Over the range of measured Rayleigh numbers of interest here, the recommended correlations are

$$Nu = 0.480Ra_D^{0.25}, \text{ For } 2 \times 10^5 \leq Ra_D \leq 2 \times 10^7 \text{ And (1a)}$$

$$Nu = 0.125Ra_D^{0.333}, \text{ For } 2 \times 10^5 \leq Ra_D \leq 2 \times 10^7 \text{ (1b)}$$

with a given uncertainty of $\pm 5\%$. (Churchill and Chu 1975) developed a correlation for a wide range of Raleigh numbers,

$$Nu = \left[0.60 + 0.387 \left\{ \frac{Ra}{[1 + (0.559/Pr)^{9/16}]^{16/9}} \right\} \right]^2, 10^{-5} \leq Ra_D \leq 10^{12} \text{ (2)}$$

Experiment uncertainty was provided. (Lienhard 1973) obtained a correlation for laminar convection from a balance of the buoyant and the viscous forces of an arbitrarily shaped immersed isothermal body,

$$Nu = 0.52Ra_\ell^{0.25} \text{ (3)}$$

Where the length scale is equal to the distance that a fluid particle travels in the boundary layer on the body. For the horizontal cylinder, $\ell = \pi D/2$

Heat transfer in two-dimensional tilted rectangular enclosures with differentially heated surfaces has been studied for $10^3 \leq Ra \leq 10^6$ (Ozoe et al 1975, Sundstrom et al 1996, Canaan et al 1996 Keyhani et al 1995, Keyhani et al 1996). Similar to the large scale circulating pattern sketched in **Fig.2**, the dominant flow is a stable circulating flow that rises along the heating wall, turns and then sinks along the cold wall. A vertical temperature gradient can develop in the core region of the tilted enclosure. For $Ra \geq 10^5$ instabilities in the flow have been found (Hart and J.E. 1971).

Most studies of heat transfer from enclosed bodies, including horizontal tube bundles, consider cases where the bounding walls drive the convective heat transfer for example, (Sparrow et al 1983, Warrington et al 1981, Farrington et al 1986, Farrington et al 1986).

Experimental studies of smooth tubes, finned tubes, and coiled tubes immersed in vertical storage tanks have yielded heat transfer correlations in the form $Nu = C Ra^n$ (Farrington et al 1986, Khalillolahi et al 1986). More analogous to the combined ICS/ heat exchanger are studies of transient natural convection in vertical enclosures with an immersed heat source or sink (Khalillolahi et al 1986).

As a first step toward developing appropriate heat transfer correlations, the heat transfer coefficient from a single horizontal finned tube in a tilted water-filled enclosure has been measured in the present work. The temperature field within the enclosure is described using local temperature measurement. These results provide a base case for a solar water heating system with a heat exchanger immersed in integral collector storage

APPARATUS

The collector is a rectangular stainless steel enclosure with inside dimensions of 121.9 cm (width) \times 94.0 cm (length) \times 10.2 cm (depth) tilted at $(30^\circ c)$ with respect to horizontal **Fig.3**.

The top side of the enclosure is a removable door to which the heat exchanger and instrumentation are mounted (3mm diameter) for insertion of the thermocouples are located in the door and along the bottom face. Additional ports are used to fill and drain the enclosure.

A uniform heat flux boundary condition that simulates solar irradiation during charging is provided by heater attached to the top face of the enclosure.

As indicated in **Fig.3**, temperatures in the enclosure were measured along the length (z-axis), width (x-axis) and depth (y-axis) by using copper-constantan thermocouple.

The immersed heat exchanger, shown in **Fig.4**, is 100.6 cm long and inner and outer diameters are respectively (19 mm) and (23mm) also the inner and outer diameter for the fins are respectively (23 mm) and (25 mm), elbows and two 11 cm long vertical brass tubes .The total length of the heat exchanger is 128.4 cm.

Water temperatures surrounding the tube were measured with four thermocouple probes placed at 90° increments, 1.1 cm from the outside wall of the tube **Fig.5**.

A constant temperature flow to the heat exchanger was maintained by the cold water supply, which includes four electric water heaters to precondition the inlet water and a large water storage tank. The flow rate was controlled with a gate valve at the outlet of the heat exchanger.

Temperatures, mass flow rate, and power input to the resistance heaters are recorded every 10 minute.

EXPERIMENTAL APPARATUS AND PROCEDURE

Thirteen transient experiments, described in table 1, were conducted over a range of tube flow rates and levels of simulated insulation .Charge ,discharge and combined charge /discharge modes with isothermal and stratified initial conditions were investigated .The experiments were begun with the insulated enclosure filled with hot quiescent water($\approx 65^\circ c$).During the discharge experiments (Nos.1 to 5) water at constant inlet temperature of ($25^\circ c$) flowed through the tube .Flow rates of 0.015,0.030 and 0.050 kg/s were studied .The experiments were continued until water in the enclosure cooled to about ($30^\circ c$).The combined charge/discharge experiments (Nos.6 to 12) were conducted in the same manner except a uniform heat flux was applied to the top face of the enclosure .These experiments were terminated after 10 hours. The charging experiment (No.13) was conducted without flow through the tube .It was terminated when fluid at the top of the enclosure reached ($90^\circ c$).

DATA ANALYSIS

The data analysis was carried out assuming that the natural convection process is quasi-steady. At each time step, the overall heat transfer rate of the heat exchanger tube was determined from measured values of mass flow rate and temperature rise.

$$Q = m \cdot c_p (T_{out} - T_{in}) \quad (4)$$

Water properties were evaluated at the average of the inlet and outlet bulk temperatures. The overall natural convection film coefficient was determined from

$$h = \frac{Q}{A \Delta T_{nc}} \quad (5)$$

Where

$$\Delta T_{nc} = T_\infty - T_w \quad (6)$$

The value of T_w used in eq. (6) is the average of the wall temperatures at top and bottom of the tube at the mid -point of its length in the flow direction (thermocouple Nos.26 and 27 in **Fig.5**) T_∞ was calculated from thermocouples are (T_{22} , T_{23} , T_{24} and T_{25}), the Nusselt and Rayleigh numbers at each time step are determined as

$$Nu = \frac{hD}{k}, \quad (7)$$

$$Ra = \frac{g \beta D^3 \Delta T_{nc}}{\nu \alpha} \quad (8)$$

Fluid properties are calculated at the film temperature equal to the average of T_w and T_c . The Nusselt numbers and the Rayleigh numbers are correlated in the form of $Nu = C Ra^n$ using statistical software package. Although there are a number of possible choices for the characteristic length, the data for the single finned tube are found to be well correlated using outer tube average diameter.

RESULTS AND DISCUSSION

Measurement of temperature distribution in the enclosure is presented first. The formation of an appropriate temperature difference that drives free convection is discussed. Correlations for the overall heat transfer coefficient in terms of the Nusselt and Rayleigh numbers are then developed. They compared to existing correlations for a single tube in an enclosure to determine the effect of the enclosure for the fin of the tube.

TEMPERATURE DISTRIBUTIONS WITHIN THE ENCLOSURE

Discharge of an initially isothermal enclosure –Results from experiment No.1 to No.3 establish the time –dependence of temperature for an initially isothermal enclosure. Data for experiment No.1 are presented in **Fig.6** to **Fig.8**. **Fig.6** includes data obtained from all thermocouples in the enclosure as a function of time; for the duration of the experiment, temperatures are spatially uniform except near the tube and the lower wall of the enclosure. The maximum difference in water temperature within the enclosure is less than $3^\circ C$. Most measurement are within $1^\circ C$.

A closer look at the temperatures near the tube for one 30 minute period beginning at $t=2$ hours is shown in **Fig.7**. The data indicate the existence of slightly hot zone above the tube and a cold plume sinking from the tube. After two hours, the water 1.1 cm on either side of the tube (thermocouples Nos.23 and 25) is $1.5^\circ C$ cooler than that of the region above the tube (thermocouples Nos.21 and 22) and $2.4^\circ C$ warmer than the water just below the tube (thermocouples Nos.24). Additionally, the temperatures at the sides of the tube are on average $2^\circ C$ above those measured in the middle and bottom portions of the enclosure. The fluid temperatures at the top, sides and bottom of the tube retain their relative values over the entire 11.5 hours of experiment No.2.

Readings of the seven thermocouples (Nos.11 to 17) along the horizontal line in the mid y-z plane ($x=0$) are plotted in **Fig.8** for the same 30 minute period as that of **Fig.6**. The water along the bottom surface of the enclosure is slightly colder than the bulk of the fluid in the enclosure. The maximum temperature difference between the reading of the thermocouple located closest to the bottom (No.17) and the average of the other six thermocouples (Nos.11 to 16) is less than $2^\circ C$, and the average difference was $1^\circ C$. Based on this difference, we infer that cold water sinking from the tube flows along the bottom of the enclosure.

Charge with no heat transfer –Heating during charging results in high degree of thermal stratification in the absence of heat transfer to the tube. The effect of applied heat flux is demonstrated in experiment No.13, in which the initially isothermal enclosure become thermally stratified when $920 W/m^2$ was applied to the top face of the enclosure. Water temperatures along the mid y-z plane ($x=0$) are plotted in **Fig.9** for the seven -hour experiment. After seven hours, a temperatures difference of $47^\circ C$ existed between positions $z = 4.4$ cm (thermocouples No.21) and $z = 87.6$ cm (thermocouple No.7).

Discharge of initially stratified enclosure- In experiments Nos.4 and 5, effect of the initial thermal stratification on the temperature distributions in the enclosure was investigated. The level of stratification is characterized by a factor suggested by (Wu et al 1987) equal to the mass weighted mean square temperature divided by the total mass of fluid in the volume considered:

$$ST = \frac{\sum_i m_i (T_i - T_{avg})^2}{\sum_i m_i} \quad (9)$$

Fig.10 shows the temperature measured during experiment No.4 with the nine thermocouples located in the mid y-z plane in the enclosure ($x = 0$). At the beginning of this experiment, the top one-third of the enclosure was filled with 65°C water and the bottom one-third was filled with 29°C water. During the filling process, the enclosure developed a stratified zone in the vicinity of the tube. The initial ST is 31.1 K^2 , based on the topmost one-sixth of the enclosed water volume ($0\text{ cm} \leq z \leq 15.2\text{ cm}$). As the experiment proceeded, temperature measurement indicates that a relatively cool flow sinks from the tube and flows down the rear surface of the enclosure. After one hour of operation, this wall plume cools the upper region and middle region of the enclosure between $z = 0\text{ m}$ and $z \sim 0.7\text{ m}$. It plunges to the relatively cold lower region between $\sim 0.7\text{ m}$ and $\sim 0.9\text{ m}$ and heats the water in the region. Early in the discharge process, the circulating flow is constrained to lie above the colder fluid near the bottom of enclosure. As the discharge process continues, the region that is colder than the plume becomes an increasingly smaller fraction of the enclosure volume.

In experiment No.5, the top half of the enclosure was filled with 65°C water and the bottom one-fourth was filled with 49°C water. After the filling process, the fluid in the region near the tube was nearly isothermal; the initial St equals 2.7 K^2 . Water temperatures are plotted in **Fig.11** as a function of time. Similar to experiment No.4, for which the initial ST is much greater, the wall plume cools the upper region of the enclosure (0 m to $\sim 0.6\text{ m}$ from the top) and heats the middle region ($\sim 0.6\text{ m}$ to $\sim 0.7\text{ m}$ from the top). Compared with experiment No.4, the region cooled by the wall plume is larger and the not heated any region because of the relatively hot water in the middle and bottom portions of the enclosure. The momentum of the wall plume is most likely less due to the smaller temperature difference between the plume and the surrounding water. The circulating flow formed by the wall plume rapidly grows with time and moves toward the bottom of the enclosure. After an hour of operation, the enclosure is isothermal from $z \sim 0.15$ to $z \sim 0.8$. Once the enclosure becomes isothermal, it remains so except for a small warmer zone above the tube.

Combined charge/discharge of an initially isothermal enclosure – In the combined charge/discharge experiments, the level of stratification in the enclosure is determined by the strength of the cold sinking plume relative to that of a warm buoyant wall flow on the front face. In the region near the tube, the applied heat flux promotes stratification. The degree of stratification near the tube is higher than that in the previously described discharge experiments with an initially isothermal enclosure.

For experiment No.9 for which the applied heat flux was 960 W/m^2 , the center portion of the enclosure ($0.2\text{ m} \leq z \leq 0.8\text{ m}$) is nearly isothermal. On the other hand, water near the tube is stratified at the beginning of the experiment and remains so for the duration of the experiment. **Fig.12** shows the water temperature near the tube for 30 minutes after two hours of operation. The temperature of water at the sides of the tube (thermocouples Nos.23 and 25) is 5.3°C lower than that of the region above the tube (thermocouples No.22 to 21) and 4.7°C higher than that of the sinking cold plume (thermocouples No.24). It is 1°C higher than the temperature measured by the (thermocouples No.20). Thus, as opposed to the isothermal discharge experiments, in this case, the temperature measured by the (thermocouples No.20) does not correctly represent the oncoming temperature that characterizes natural convection.

Combined charge/discharge with an initially stratified enclosure – Temperatures measured in the combined charge/discharge experiment with initial thermal stratification (experiment No.12 with an initial $ST = 14.1\text{ K}^2$) are plotted in **Fig.13**. The temperature distributions along the length of the enclosure indicate that the cold plume sinking from the tube descends into the enclosure until it is neutrally buoyant. Because the plume cannot fully penetrate the lower cold region of the enclosure, the

circulating flow gradually extends to the bottom of the enclosure as energy is removed .In the isothermal region ,the effect of the cold plume on the overall structure of the flow tends to dominate that of heat input on the front face ,as can be seen by the nearly constant temperatures over the middle portion of the enclosure for $0.5 < t < 10$ hr .In the portion of the enclosure below the isothermal region ,the enclosure remains stratified ,and the temperature increases due to the addition of heat at the front face .At the top of enclosure ,near and above the tube ,effects of heat input dominate the flow and temperature fields.

HEAT TRANSFER CORRELATIONS

Using the statistical software we get the correlation between the Nusselt number and Rayleigh

Number in form $Nu = 0.716Ra^{0.247}$, For $2 \times 10^5 \leq Ra \leq 2 \times 10^7$ (10)

As shown in **Fig.14** .Compare the present work with (Liu et al 2001) then we find the curve of present work is lower than curve of (Liu et al 2001) with the value [27%] respectively, as shown in **Fig.15**.

CONCLUSION

Measurements of water in the enclosure permit interpretation of the flow field. As energy is transferred to the tube under any level of initial stratification, a cold plume sinks from the tube and flows to the rear surface of the enclosure .This plume promotes a circulating flow that promotes overall mixing in the mid – section of the enclosure. If there is either heat input on the front face or significant initial stratification near the immersed tube, stratification will persist during the discharge process.

Measurements of water temperatures near the tube and the tube wall temperature permit calculation of a Rayleigh number during the cooling process. For $2 \times 10^5 \leq Ra \leq 2 \times 10^7$, dimensionless heat transfer coefficients are correlated by $Nu = 0.716Ra^{0.247}$.Rayleigh number is based on the temperature difference between the water temperatures near the tube and the temperature of the tube wall.

Nomenclature

A	out heat transfer area of tube, m^2
Cp	specific heat of water, $J/kg \cdot ^\circ c$
C	Empirical constant used in $Nu = CRa^n$
D	Tube average diameter ,m
h	Natural convection heat transfer coefficient, $W/m^2 \cdot ^\circ c$
i	Enclosure node at constant temperature, used in ST
k	Thermal conductivity of fluid, $W/m \cdot ^\circ c$
ℓ	Length scale used in Ra
\dot{m}	Mass flow rate in tube ,kg/s
n	Empirical exponent in $Nu = CRa^n$
Nu	Nusselt number, hD/k
Pr	Prandtl number, ν/α
\dot{Q}	Total energy transferred through the tube bundle ,W
Ra	Rayleigh number , $g \beta D^3(T_w - T_\infty)/(\nu \alpha)$
Re	Tube Reynolds number
R^2	Coefficient of determination
ST	Stratification factor ,eq.(9), K^2
t	Time ,s
T_{avg}	Average or stirred temperature of the enclosure , $^\circ c$
T_i	Water temperature at node I , $^\circ c$
T_{in}	Water temperature at the inlet of exchanger, $^\circ c$



T_{nc}	Refer to temperature difference that drives natural convection, °C
T_{out}	Water temperature at the outlet of exchanger, °C
T_w	Temperature of outer tube wall, °C
T_{∞}	Storage water temperature that drives natural convection, °C
x,y,z	Cartesian coordinates

Greek symbols

α	Thermal diffusivity, m^2/s
β	Coefficient of volumetric thermal expansion,
Δ	Refers to temperature difference, °C ⁻¹
θ	Inclination angle of the enclosure, degrees relative to horizontal
ν	Kinematic viscosity, m^2/s

REFERENCES

- Canaan, R.E., and Klein, D.E.**, "An experimental investigation of natural convection heat transfer within horizontal spent-fuel assemblies," Nuclear Technology, 116, No.3, pp. (306-318), 1996.
- Churchill, S.W., and Chu, H.H.S.**, "Correlating equations for laminar and turbulent free convection from a horizontal Cylinder." University of Pennsylvania, Journal of Mass and Heat Transfer, vol., 18, pp (1049-1055).1975.
- Farrington, R.B. and Bingham C.E.**, "Test and analysis of immersed heat exchangers," Solar Energy Research Institute, SERI Report#TR-253-2866, 1986.
- Farrington, R.B.**, " Test Results of immersed coil heat exchangers and liquid storage tanks used in the packaged systems program," Solar Energy Research Institute, SERI Report#TR-254-2841, 1986.
- Hart, J.E., "Stability of the flow in the differentially Heat inclined Box", Journal of Fluid Mechanics, 47, No.3, pp. (547-576) 1971.
- Keyhani, M.and Dalton, T.**, "Natural convection heat transfer in horizontal Rod-bundles Enclosures," Journal of Heat Transfer, 118, No.3, pp. (598-605) 1996.
- Keyhani, M.and Luo, L.**, "Numerical study of Natural convection heat transfer in horizontal Rod-bundles, "Nuclear Science and Engineering, 119, No.2, pp. (116-127) 1995.
- Khalilolahi,A.,and Sammakia,B.**, "Unsteady natural convection generated by a heated surface within an enclosure ," Numerical Heat Transfer,9,No.6, pp.(715-730), 1986.
- Lienhard, J.H.**, "On the commonality of equations for natural convection from immersed Bodies "International Journal of Heat and Mass Transfer, 16, No.11, pp (2121-2123), 1973.
- Liu, W.Davidson,J.Hand Kulacki ,F.A.**, "Natural Convection From a Single Tube Immersed in a Tilted thin Enclosure "Proceedings of International Conference on Energy Conversion and Application(ICECA'2001),Huazhong University of Science and Technology Press,1.PP(408-413), Wuhan,China,2001.
- Morgan, V. T.** "The overall convective Heat Transfer from smooth Circular Cylinders "Advances in Heat Transfer , Hartnett ,J.,and Trivine, T. Tr. ,Eds., vol.,11, Wiley. Interscience, New York, pp (199-264).1975.
- Ozoe ,H.,Sayama ,H.,and Churchill,S.W.**, " Natural convection in an inclined Rectangular channel at various Aspect Ratios and Angles-Experimental Measurements," International Journal of Heat and Mass Transfer,18,No.12, pp.(1425-1431) ,1975.

Sparrow, E.M., and Charm chi, M., “Natural convection Experiments in an Enclosure between Eccentric or concentric vertical Cylinders of Different Height and Diameter “University of Minnesota state, Journal of Mass and heat transfer, vol.20, NO.1. pp (133-143). 1983.

Sundstrom, L.-G., and Kimura, S., "On laminar free convection in inclined rectangular enclosures,"", Journal of Fluid Mechanics, 313, pp. (343-366), 1996.

Warrington, R. O., and Crupper, G.,”Natural convection Heat Transfer between Cylindrical tube Bundles and a Cubical Enclosure “, University of Minnesota state, Journal of heat transfer, vol.103, February, pp (103-107), 1981.

Wu,L.,and Bannerot,R.B. "Experimental study of the effect of water extraction on thermal stratification in storage ,"Solar Engineering,1,pp(445-451) ,1987.

Table 1.Experimental operating conditions

Run No.	Operating Mode	Initial ICS Temperature (° c)	Nominal m° (kg/s)	Re	T_{in} ° c	Heat Flux (W/m ²)	Ra	Nu	Δ_t (hr)
1	Discharge	62	0.015	1133~1306	25	0	$2 \times 10^5 \sim 9.75 \times 10^6$	15 ~ 33	11.5
2	Discharge	70	0.03	2267~2584	25	0	$4.9 \times 10^5 \sim 1.9 \times 10^7$	17.6~42.7	10.8
3	Discharge	75	0.05	3779~4214	25	0	$4.1 \times 10^5 \sim 2 \times 10^7$	17.6 ~ 46	10.0
4	Discharge	Stratified Top at 65 Bottom at 29	0.05	3774~3952	25	0	$3.4 \times 10^5 \sim 9.7 \times 10^6$	16.7 ~ 39.5	4.3
5	Discharge	Stratified Top at 65 Bottom at 48	0.05	3774~4076	25	0	$4.5 \times 10^5 \sim 8 \times 10^6$	17.6 ~ 40	9.0
6	Charge/Discharge	64	0.03	2420~2581	25	260	$4.5 \times 10^5 \sim 8 \times 10^6$	25 ~ 38.6	10.0
7	Charge/Discharge	67	0.03	2420~2581	25	480	$1.9 \times 10^6 \sim 1.15 \times 10^7$	27.7 ~ 41.9	10.0
8	Charge/Discharge	75	0.03	2445~2687	25	700	$2.12 \times 10^5 \sim 1.23 \times 10^7$	31 ~ 42	10.0
9	Charge/Discharge	62	0.03	2445~2609	25	960	$3.38 \times 10^6 \sim 1.2 \times 10^7$	33.5 ~ 41	10.0
10	Charge/Discharge	68	0.15	1276~1370	25	920	$4.16 \times 10^6 \sim 9.37 \times 10^7$	30 ~ 38	10.0
11	Charge/Discharge	61	0.05	3912~4119	25	920	$4.8 \times 10^6 \sim 1.3 \times 10^6$	32 ~ 37	10.0
12	Charge/Discharge	Stratified Top at 81 Bottom at 44	0.03	2420~2661	25	920	$4.47 \times 10^6 \sim 8.19 \times 10^7$	34.5 ~ 49	10.0
13	Charge	27	0	No flow	25	920	-	-	7.0

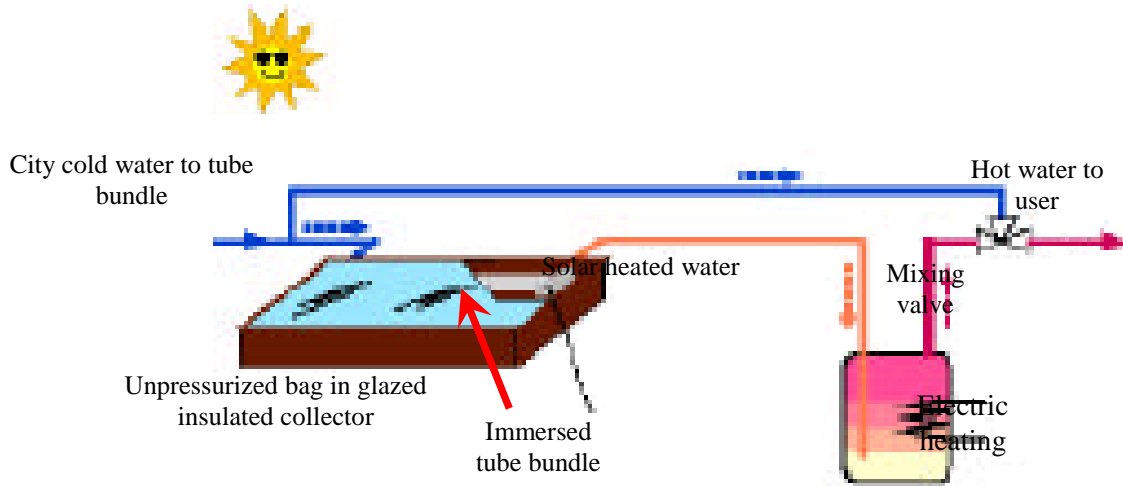


Fig (1). Conceptual system for a low cost collector and a load-side heat exchanger

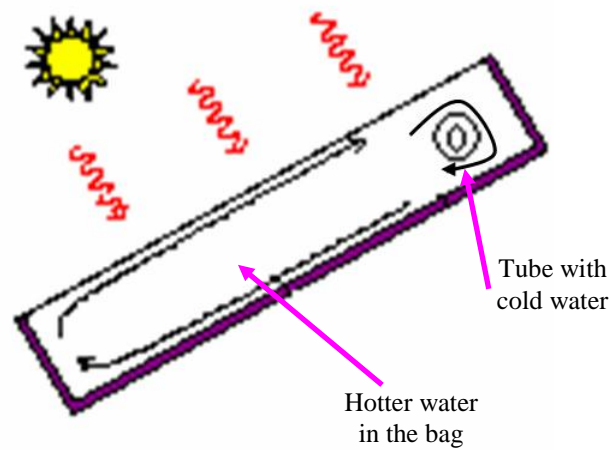
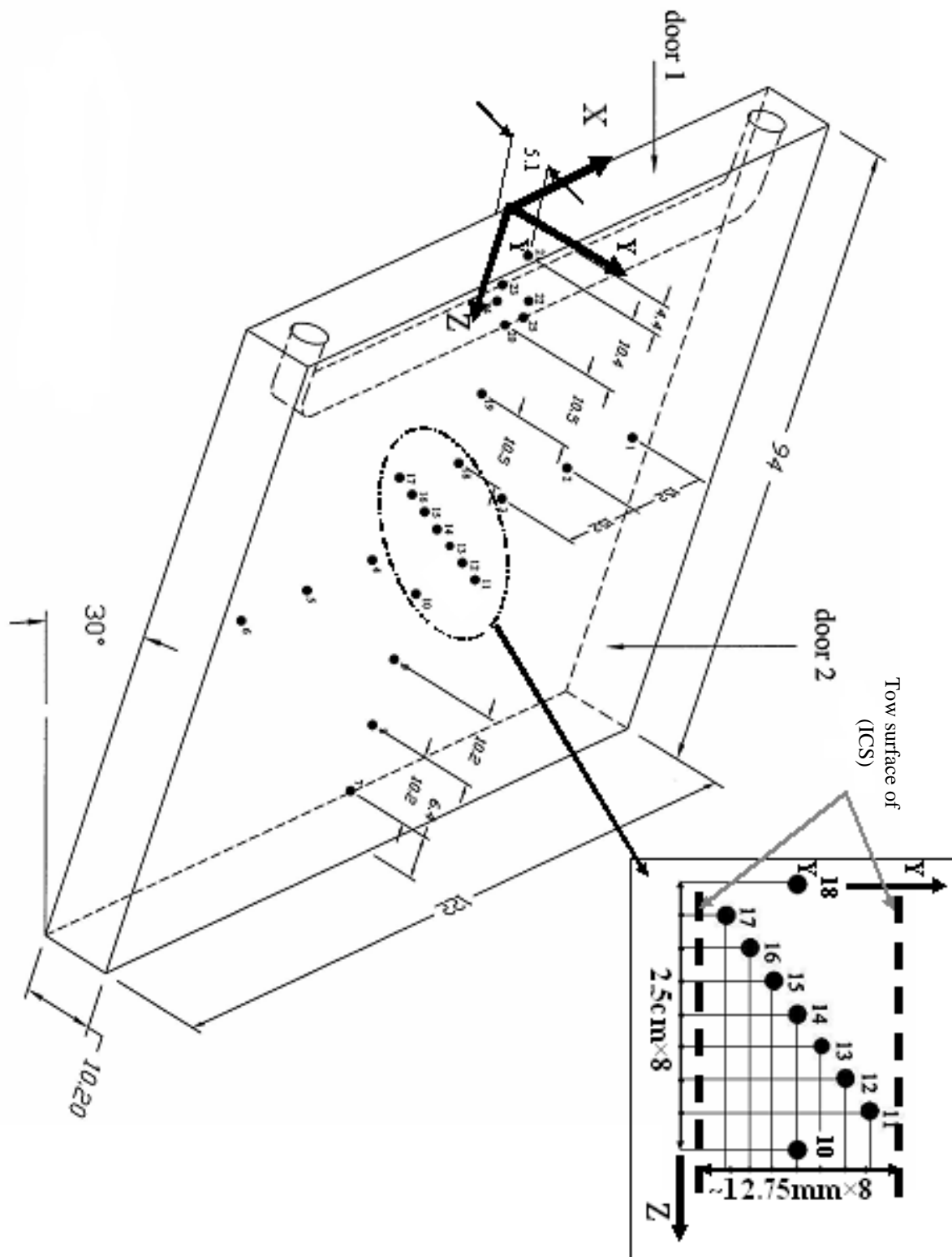


Fig (2). Buoyancy driven flow inside the inclined solar collector with an immersed heat exchanger

Fig (3). Enclosure and locations of thermocouples
Note: All dimensionsin (cm)



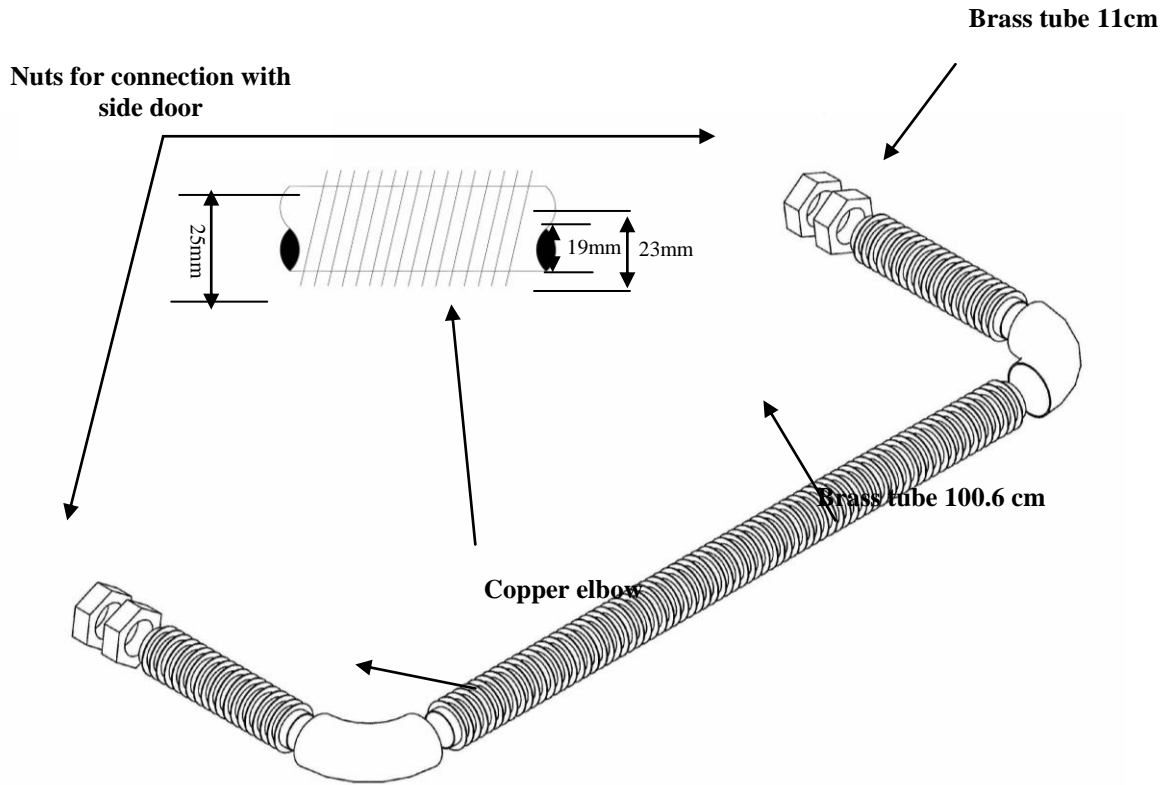


Figure (4). Finned Tube (Heat Exchanger)

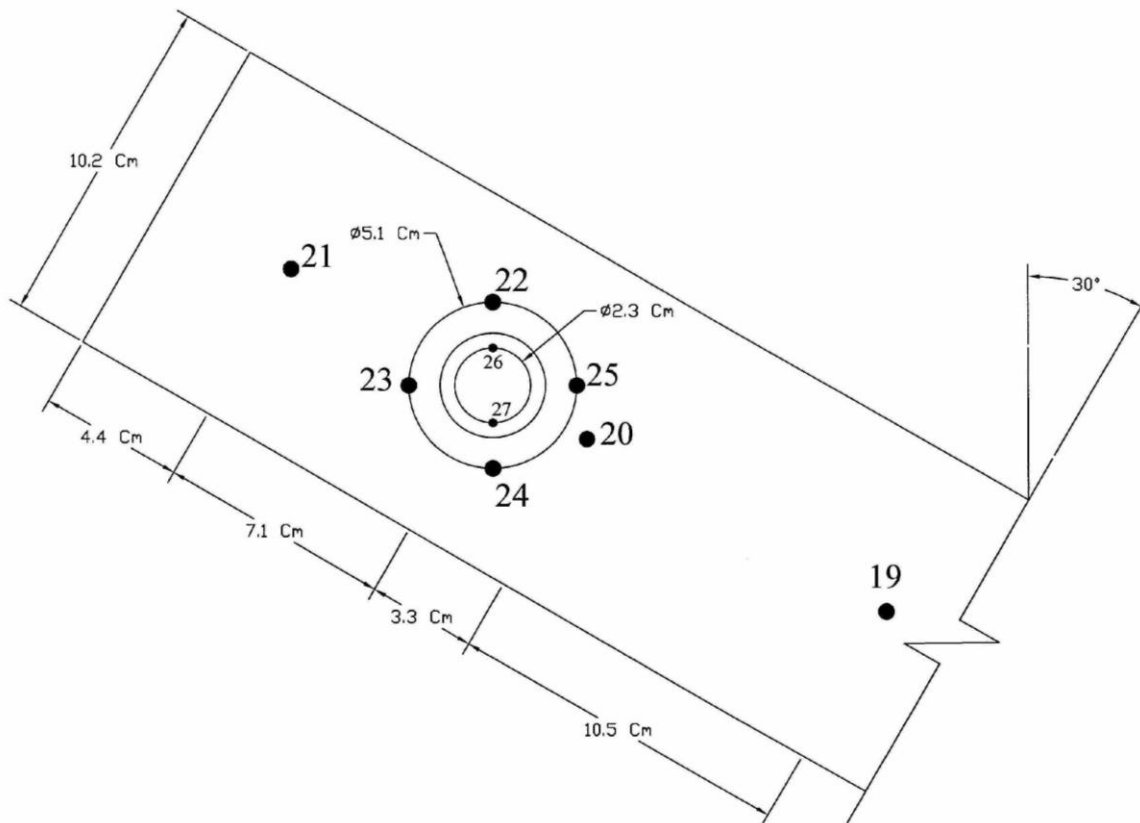
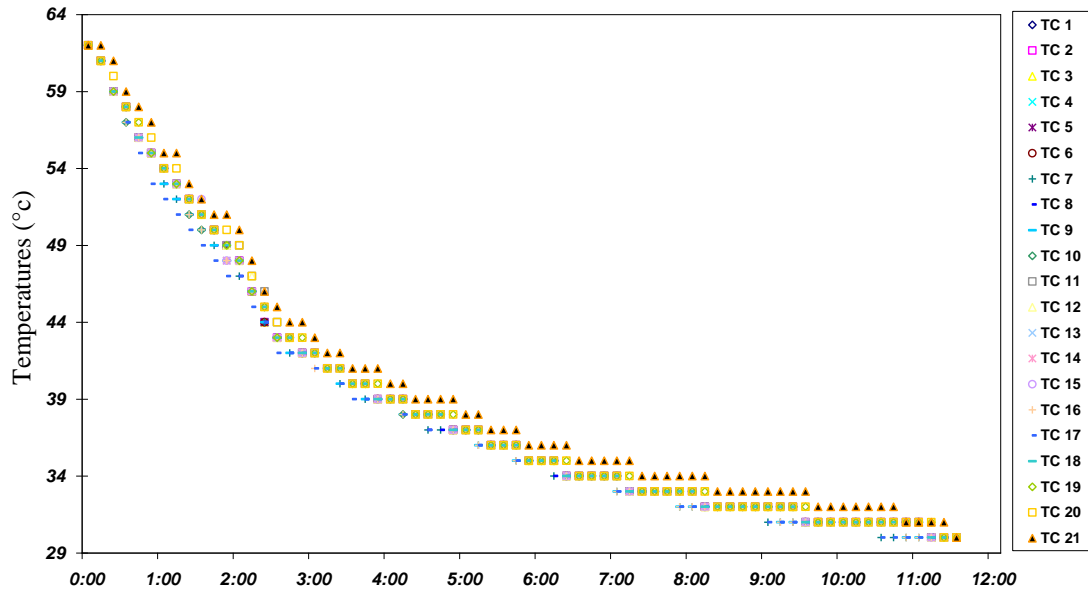


Fig (5). The thermocouples around the heat exchanger

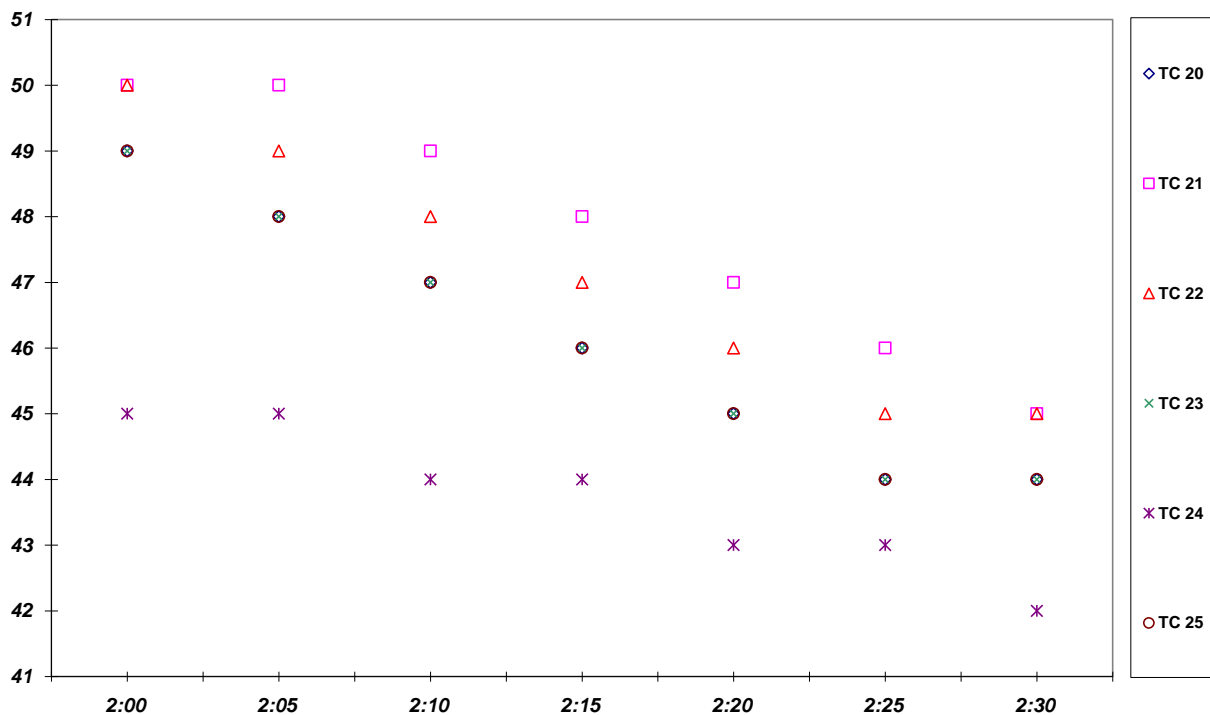
Time (h:m)

Fig (6). Water temperatures inside the enclosure for experiment No.1



Time (h:m)

Fig (7). Water temperatures in the top portion of the enclosure over a 30 minute interval during experiment No. 1



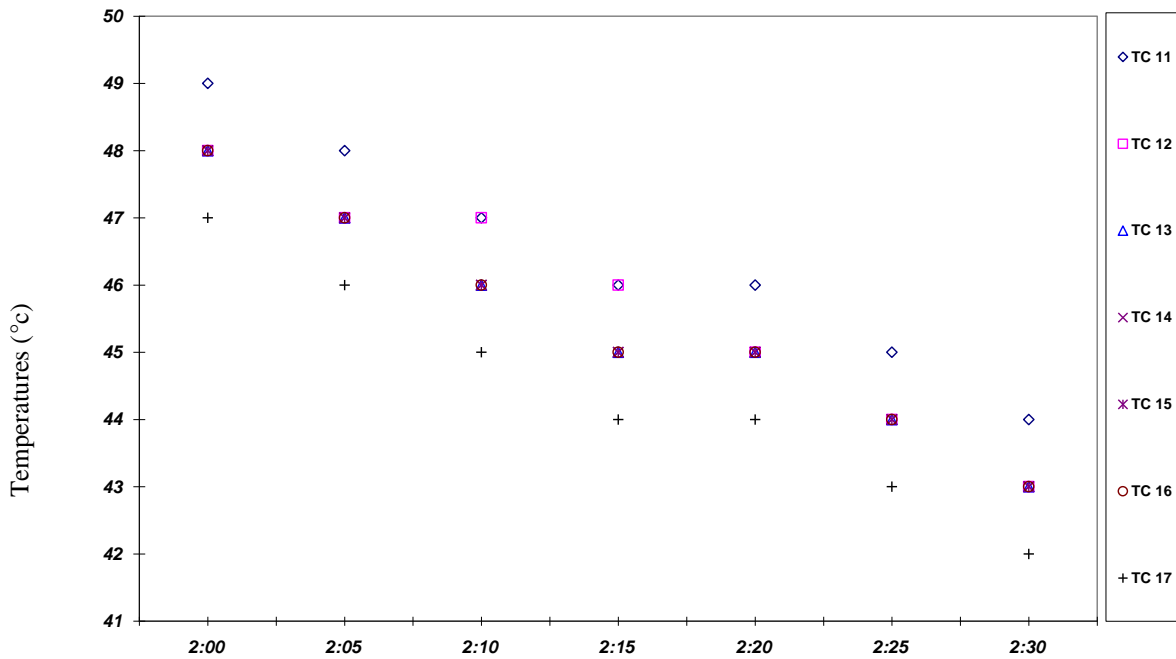
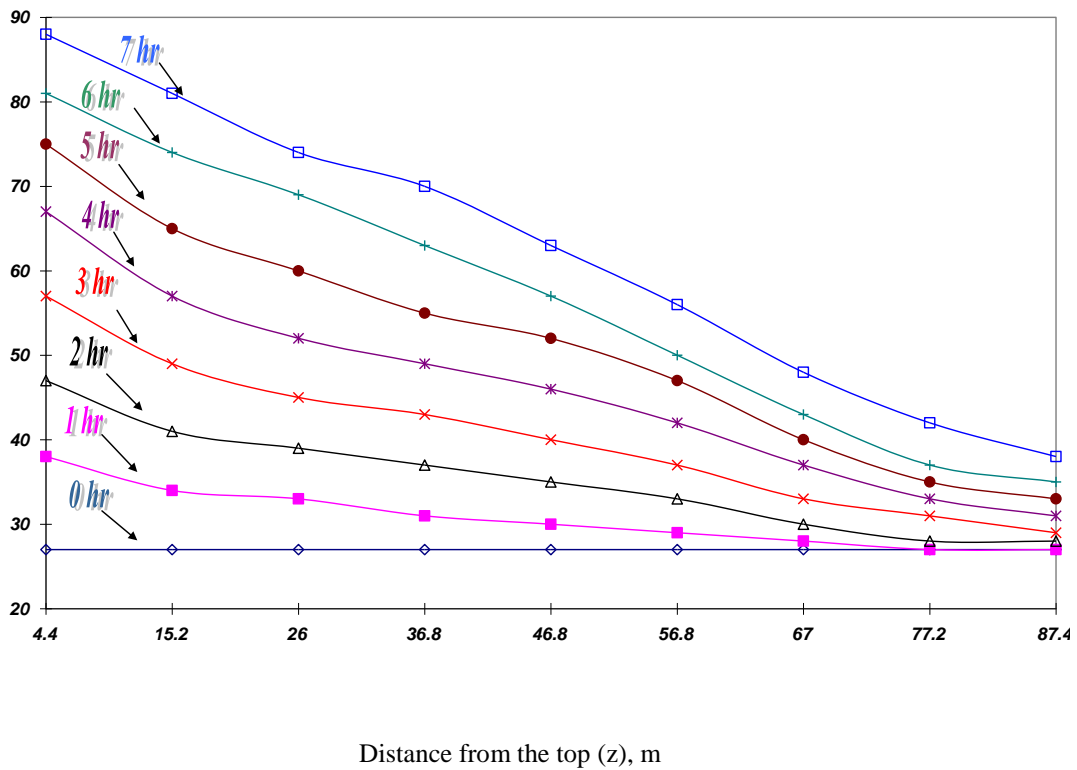


Fig (8). Water temperatures distribution along the horizontal line in the mid y-z plane over a 30 minute interval in experiment No.1



Distance from the top (z), m
Fig (9). Hourly water temperatures distribution in the enclosure during the charging experiment No.13

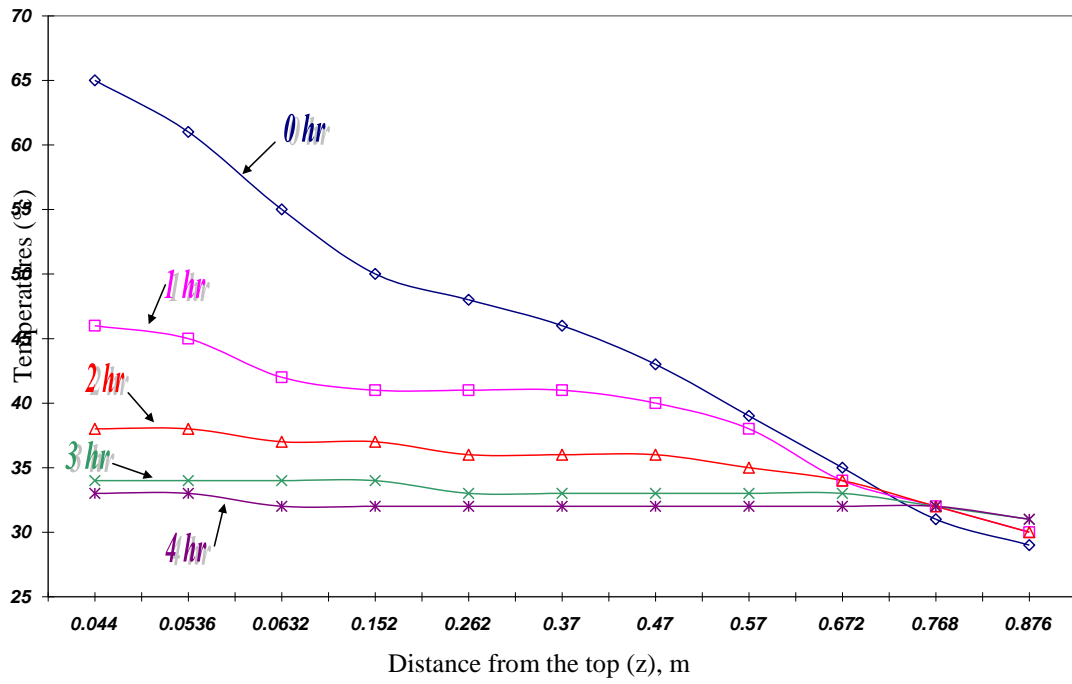


Fig (10). Hourly water temperatures distribution in discharging experiment No.4

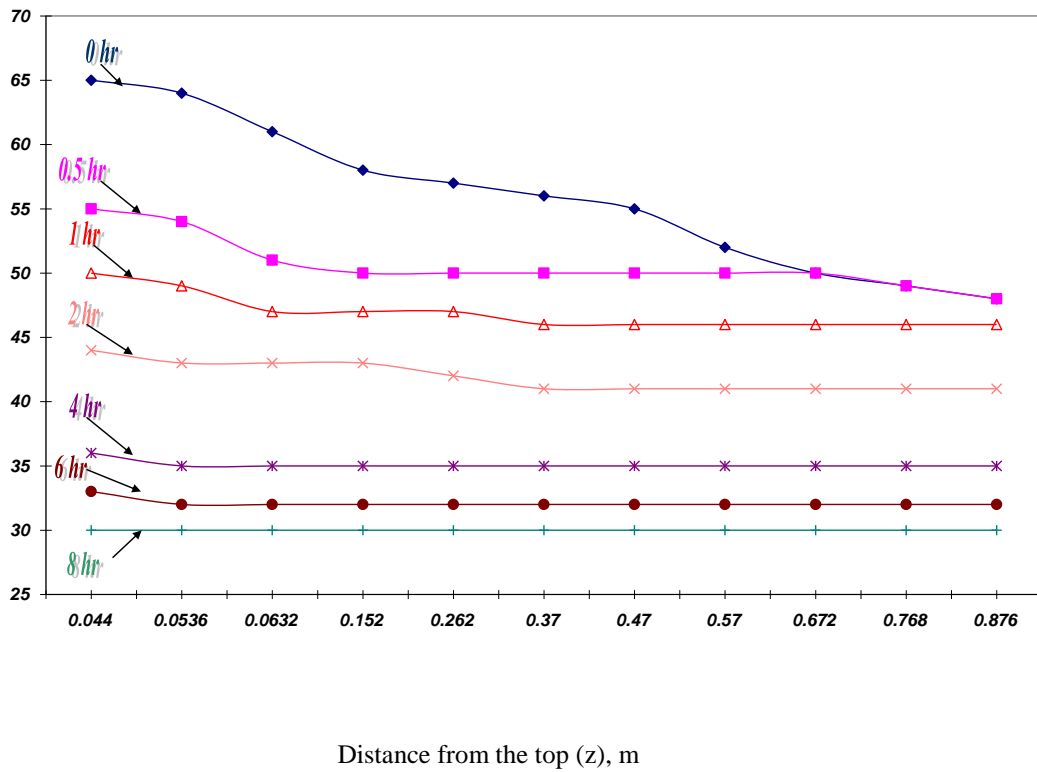


Fig (11). Hourly water temperatures distribution in discharging experiment No.5

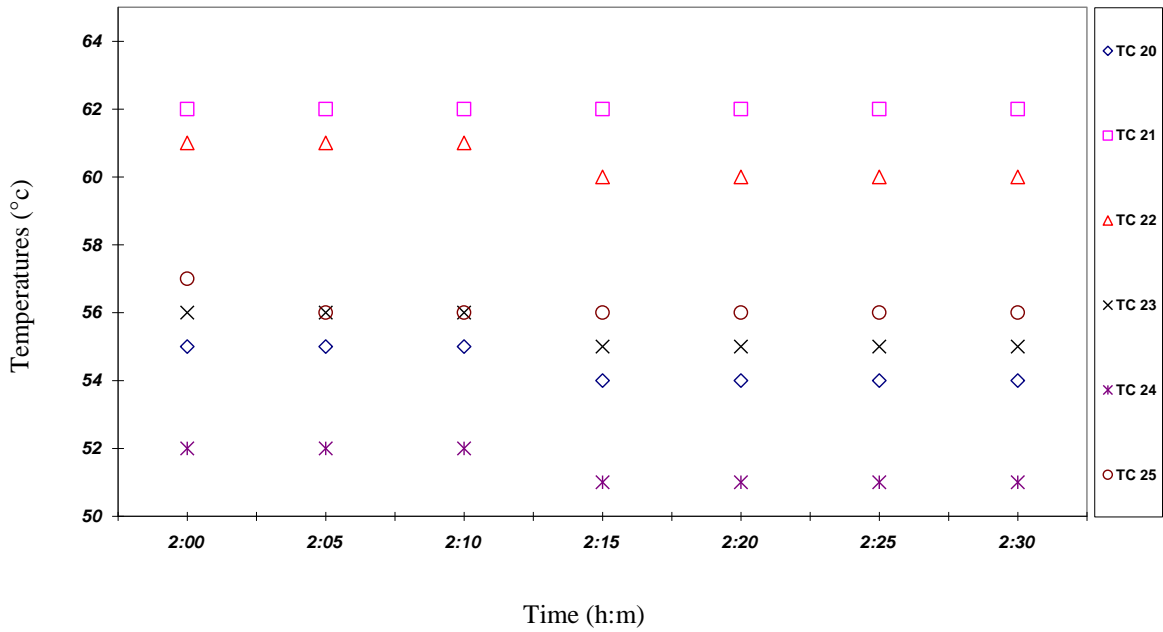


Fig (12). Water temperatures in the top portion of the enclosure over a 30 minute interval during experiment No. 9

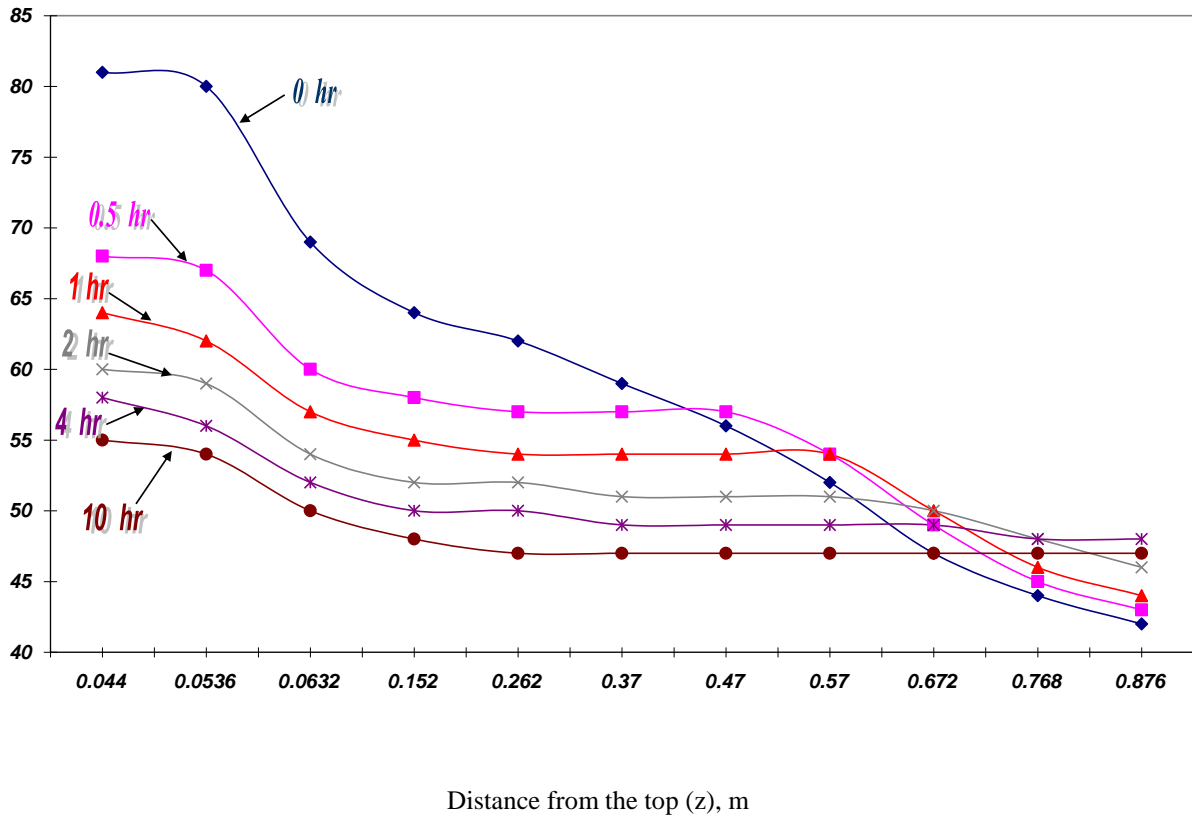
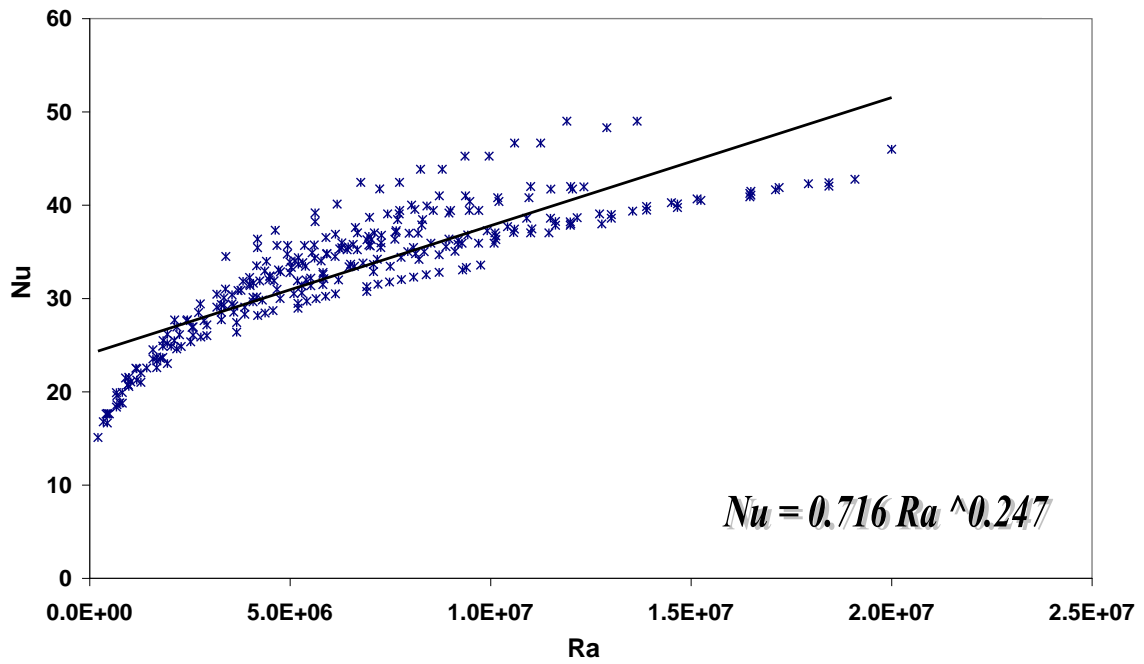


Fig (13). water temperatures distribution in the mid y-z plane in combined charge/discharging experiment No.12



Fig(14). Nusselt number correlation and measured values for experiments 1-12.

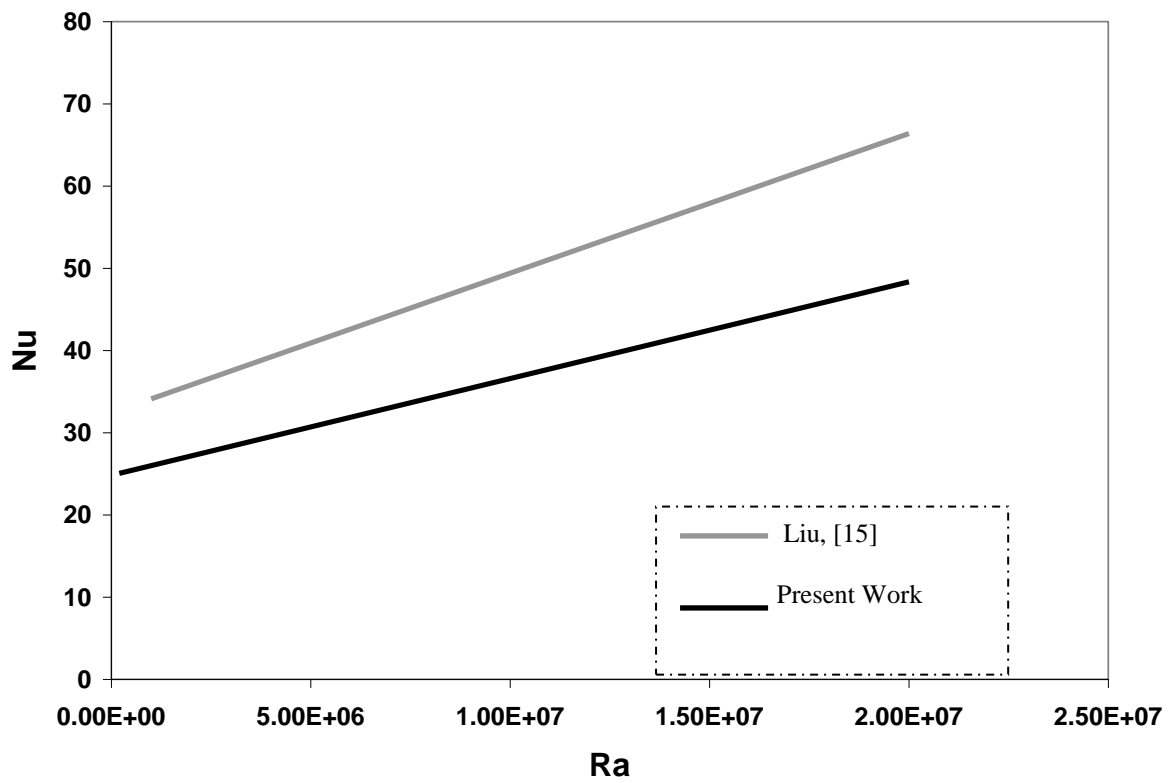


Fig (15).Comparing of the result